

Shearing Apparatus for Neutron Scattering Studies on Fluids: Preliminary Results for Colloidal Suspensions

G. C. Straty,^{1,2} H. J. M. Hanley,¹ and C. J. Glinka³

Received November 21, 1989; final April 15, 1990

A Couette-type concentric cylinder apparatus to investigate liquids at equilibrium and under shear has been constructed and tested. The apparatus is designed for a neutron facility and is optimized as a general purpose adjunct to the small-angle neutron scattering (SANS) equipment. It is versatile and rugged; a wide range of shear rates and operating temperatures can be covered; and controls are fully automated. Test results with sheared colloidal suspensions of 91-nm polystyrene spheres are presented. Evidence of shear-induced structure changes is clear.

KEY WORDS: Colloidal suspension; Couette flow; neutron scattering; SANS; shear-induced melting; shearing cell.

1. INTRODUCTION

We have constructed a Couette-type shearing cell to be used in a neutron facility. The purpose of this paper is to outline the apparatus. Some test results on a sheared colloidal suspension from the 8m SANS (small-angle neutron scattering) equipment at the NIST (National Institute of Standards and Technology) reactor facility are reported.

Topical interest in the distortion of the intermolecular microstructure of a sheared fluid was the motivation to build the shearing cell, and neutrons are a valuable probing radiation for fluids. The radiation

Work carried out at the National Institute of Standards and Technology, not subject to copyright.

¹ Thermophysics Division, National Institute of Standards and Technology, Boulder, Colorado 80303.

² To whom correspondence should be addressed.

³ Reactor Radiation Division, National Institute of Standards and Technology, Gaithersburg, Maryland 20899.

wavelength λ is compatible with the characteristic dimension of a fluid. The magnitude Q of the scattering wave vector for neutrons is given by

$$Q = (4\pi/\lambda) \sin(\theta/2) \quad (1)$$

where θ is the scattering angle and $Q = k_0 - k_1$, where k_0 and k_1 are the incident and scattered wave vectors, respectively, of the radiation. The Q range for the NIST reactor facility SANS at present is about $0.003 < Q < 0.5 \text{ \AA}^{-1}$, which corresponds roughly to characteristic dimensions of 2–2000 \AA in the fluid.

An attractive feature of neutrons is that materials such as fused quartz and aluminium, as well as atmospheric dust and dirt, are transparent for values of Q relevant to liquids. We can thus build a robust apparatus—for example, the shearing cell—and not have to be unduly concerned with optical access and cleanliness.

2. APPARATUS

The apparatus is a Couette-type concentric cylinder fused quartz sample cell coupled to a computer-controlled drive mechanism and a computer-controlled thermostat system.^(1,2) Neutrons are scattered from the fluid in the annular gap between the cylinders; see Fig. 1A. Thermostating fluid can be circulated within the inner stator, but is excluded from the neutron path by the sealed cross tube; see Fig. 2. The outer cylinder is driven by a microprocessor-controlled DC servo motor that can be programmed for any desired combination of velocity, acceleration, delay time, direction of motion, or rotation angle. We have verified that these variables can be programmed to be precise to within 0.1% for at least 24 hr of continuous operation. The motor can deliver a torque of approximately 3 N m at 5400 RPM. A personal computer interfaces the motor and thermostating controls with the operating and data acquisition system of the SANS spectrometer, so that full automation of the experiment can be achieved if necessary.

Since the apparatus is to serve a user community, ease of use, versatility, and low cost were major design considerations. Maximum use of commercial components reduces cost and increases versatility. The vertical support columns for the apparatus are fabricated from structural elements of a type used for optical bench construction, permitting easy assembly and attachment of accessories. The novel quartz cell configuration reduces cost and allows for simple assembly and disassembly. The cell chuck has adjustments for precisely aligning the cell rotor, reducing considerably the need for the often extremely accurate machining requirements in this type of application.

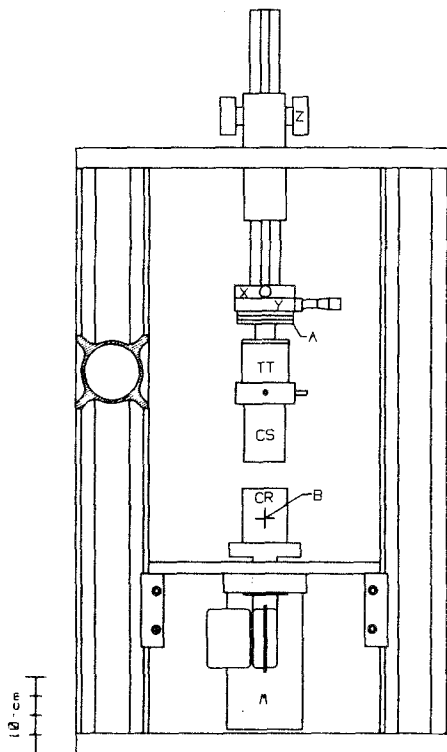


Fig. 1. Schematic drawing of the shearing apparatus. M, drive motor; CR, cell rotor; CS, cell stator; TT, torque transducer; A, alignment coupling; X and Y, micrometer adjustment screws; Z, vertical adjustment. The neutron beam is directed to point B.

In this work, the cell was constructed with a nominal mean diameter of 57 mm, and an annular gap of nominal 0.6 mm. The apparatus constant for this cell is $4.89 \text{ Hz/RPM} \pm 4\%$.

3. SHEAR-INDUCED STRUCTURE CHANGES

Solutions of 91-nm polystyrene latex spheres in deionized water were selected as candidate fluids to test the apparatus; suspensions give clear interference patterns, and the theory of scattering of neutrons from a latex is well known (see, e.g., ref. 3). We wished to ensure that the neutron scattering intensity patterns using the shearing cell with the outer cylinder stationary (that is, with fluid in equilibrium) were consistent with previous data taken by us on the SANS spectrometer⁽⁴⁾ and by Sirota *et al.* using X-rays.⁽⁵⁾ We further intended to explore shear-induced melting in a

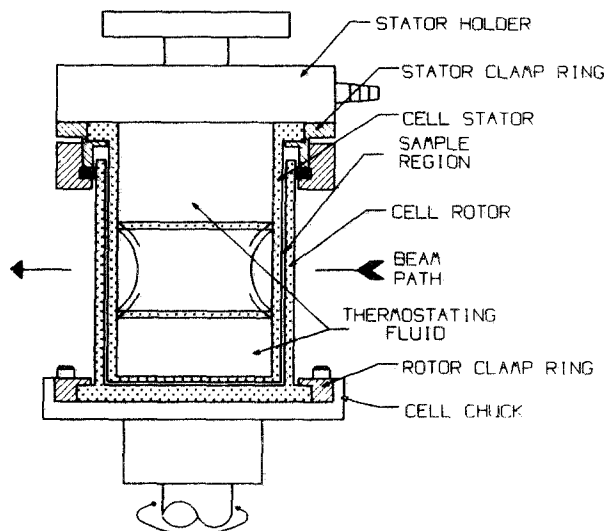


Fig. 2. Details of the shearing cell.

colloidal crystal. Light scattering experiments have indicated that the solidlike crystal structure of a latex suspension can be destroyed by subjecting the suspension to a shear,^(6,7) and a similar transformation has been observed with neutrons.⁽⁸⁾ From the viewpoint of nonequilibrium thermodynamics and statistical mechanics, the phenomenon is important in that it can be interpreted as one direct manifestation of non-Newtonian behavior in simple liquids.^(9,10) Current work on suspensions includes light scattering and neutron scattering experiments to investigate shear-induced order.⁽¹¹⁻¹³⁾

Experiments were carried out with solutions prepared from an approximately 30% mass fraction suspension of polystyrene spheres of nominal diameter 91 nm with less than 10% polydispersivity. We investigated the solution at a nominal temperature of 295 K for volume fractions (ϕ) of 0.3 and 0.085 in deionized water, and 0.06 in a deionized $\text{H}_2\text{O}/\text{D}_2\text{O}$ mixture. The suspensions were expected to be crystalline at these initial conditions.⁽⁵⁾

A schematic of the scattering geometry is shown in Fig. 3, where, in Cartesian coordinates, the gradient ∇ is in the y coordinate, the velocity v is along x , and the z coordinate is vertical.

For the SANS measurements, a seven-beam converging pinhole collimation system⁽¹⁴⁾ illuminated a circle of approximately 20 mm diameter at the sample. For an incident wavelength of 12 Å and a sample-

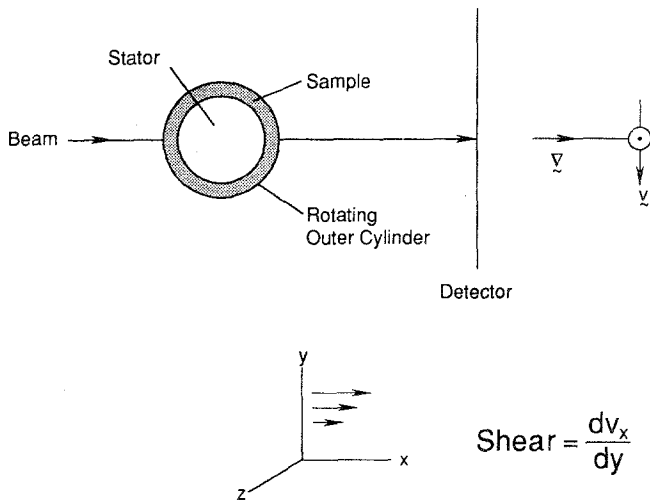


Fig. 3. Scattering geometry of the system.

to-detector distance of 3.6 m, the Q range covered by the instrument's two-dimensional position-sensitive detector was $0.003\text{--}0.06 \text{ \AA}^{-1}$.

Scattering intensities were recorded for the samples at rest with the cell stationary and under shear with the outer cylinder rotating at speeds from 0.01 to 25.0 RPS. The intensity data were corrected for the empty-cell contribution, background scattering, and sample transmission in the usual way. We verified from previous work⁽⁴⁾ that multiple scattering would be insignificant given the sample thickness here. The samples are strong scatterers, so the incoherent contribution to the scattering was taken to be negligible at the values of Q of interest.

Results and Discussion

The results are displayed here as iso-intensity plots. Figures 4 and 5 are the curves for the $\phi = 0.06$ and the 0.30 samples, respectively, for the sample at rest and when subjected to various shear rates. Similar results were observed for the $\phi = 0.085$ solution. The plots are the projections of the experimental scattering intensity in the x - z plane; see Fig. 3. The intensities have been corrected for background scattering and the empty-cell contribution, but not for the single-particle form factor.

The $\phi = 0.06$ sample is at rest in Fig. 4a. We observe six high-intensity spots at $Q \cong 0.005 \text{ \AA}^{-1}$, and evidence of six less intense spots at $Q \cong 0.010$. The location and orientation of the sixfold spot pattern are consistent with 2D close-packed layers, with the close-packed (nearest neighbor) direction

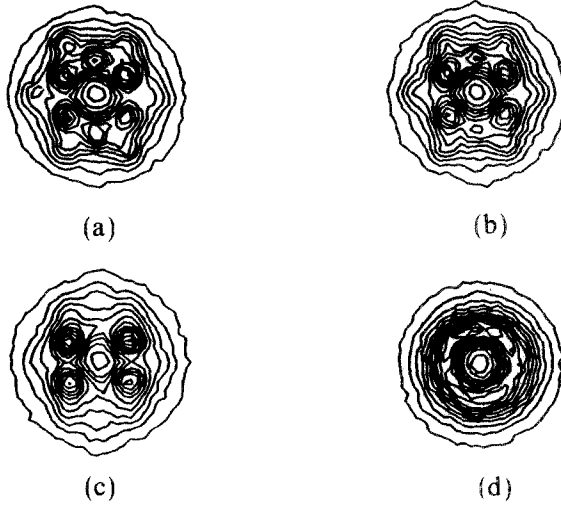


Fig. 4. Scattered intensity isointensity contours in the $x-z$ plane from the $\phi = 0.06$ sample, (a) from the system at rest; and from the system subjected to a shear rate of (b) 2.93 Hz (0.6 RPM), (c) 12 RPM, and (d) 36 RPM. See text.

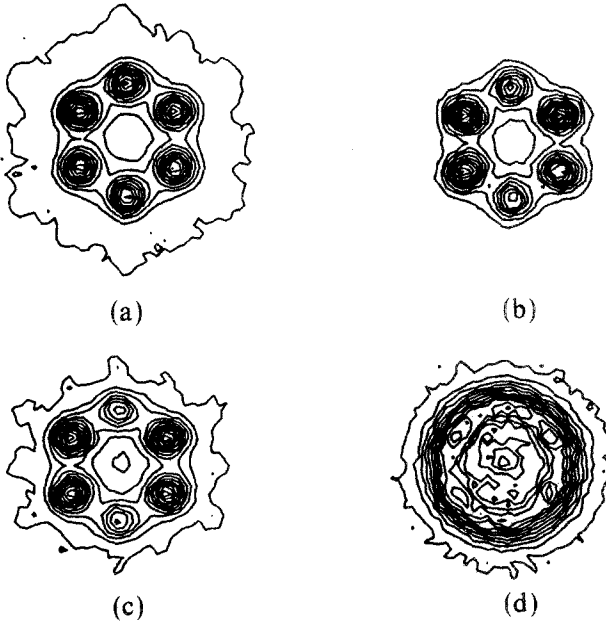


Fig. 5. Scattered intensity isointensity contours in the $x-z$ plane from the $\phi = 0.30$ sample, (a) from the system at rest; and from the system subjected to a shear rate of (b) 58.7 Hz (12.0 RPM), (c) 60 RPM, and (d) 300 RPM. See text.

along v , that are randomly stacked in the y direction. Figures 4b and 4c are typical of the intensity pattern from the sheared sample as the shear rate is increased. The suspension is subjected to a shear of 0.6 RPM (2.93 Hz) in Fig. 4b and 12 RPM in Fig. 4c. The inner sixfold symmetry weakens to a four-spot pattern with twofold symmetry, most probably because of a loss of correlation in the z direction. We surmise that this occurs because the shearing motion forces one 2D layer past another in the v direction. The intensity is liquidlike at higher values of the shear, for example, Fig. 4d for 300 RPM. The liquidlike intensity persists until the system is destroyed at a high shear. The sequence is reversible and repeatable within the resolution of the instrument.

Figure 5 displays typical intensity contours for the $\phi = 0.30$ suspension. For the suspension at rest (Fig. 5a) the scattering pattern is consistent with that from 2D hexagonally closed-packed layers, with a close-packed direction along v , which are randomly stacked in the gradient direction. Under shear (Figs. 5b and 5c) the sixfold symmetry remains, but the upper and lower spots become less intense with increasing shear, consistent with a sliding motion.⁽⁸⁾ The crystal-like structure vanishes at a sufficiently high shear and the intensity pattern is that of a liquid with some residual anisotropy (Fig. 5d).

The Sheared Liquid. Results for the sheared liquid are preliminary, but do show features that encourage further work. For example:

1. Figure 6 shows the circular averaged intensity curves corresponding

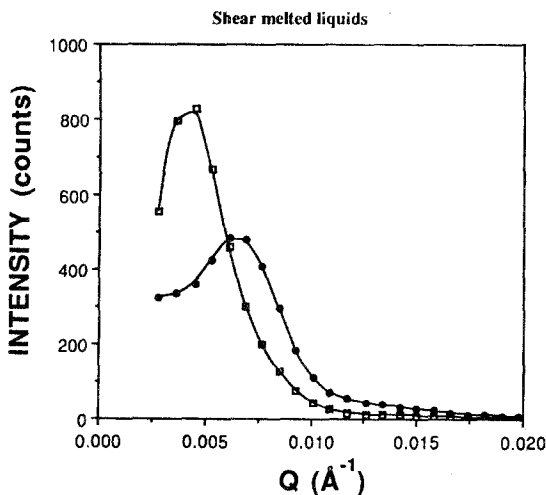


Fig. 6. Scattered intensity from the shear-melted liquid. (●) $\phi = 0.30$, 1468 Hz; (□) $\phi = 0.06$, 176 Hz.

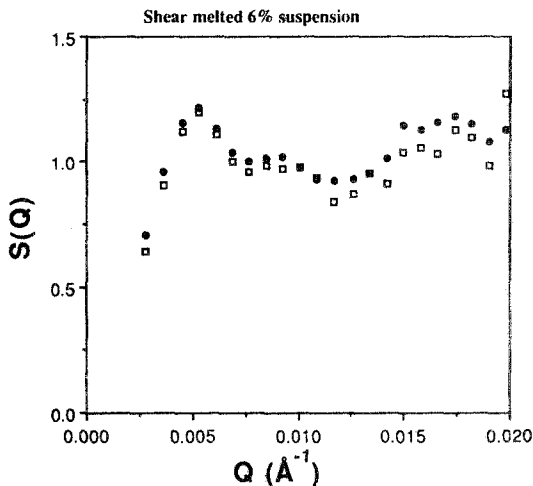


Fig. 7. Structure factors of the $\phi = 0.06$ shear-melted liquid at two shear rates, (□) 176 Hz, (●) 7338 Hz.

to Figs. 4d and 5d for the suspension in the liquidlike state. The major peak positions (the peak heights are not normalized) are at the expected values of Q , and the positions scale correctly as $\phi^{1/3}$. The curve for the $\phi = 0.30$ suspension, however, appears anomalously high at low Q .

2. Figure 7 presents the structure factor $S(Q)$ for the 0.06 suspension at the two shear rates of 36 and 1500 RPM (not shown in Fig. 5) using the form factor extracted from data of the polystyrene suspension at $\phi = 0.015$. The $S(Q)$ at 1500 RPM is uniformly higher than $S(Q)$ at 36 RPM, and the difference is outside the estimated error. That $S(Q)$ depends on the applied shear is consistent with computer simulation and recent results for a sheared liquid suspension.⁽¹³⁾ The trend, however, is that the structure factor falls with shear. Nevertheless, any shear rate effect on $S(Q)$ is significant because a departure from the equilibrium structure factor is a direct measure of non-Newtonian behavior in the fluid. It is often assumed that non-Newtonian behavior can be seen only in fluids of complex structure and would not occur in a simple suspension.

3. By comparing scattered intensities along the x and the z axes we have weak evidence of anisotropy in the shear-melted liquid. Ackerson and co-workers⁽⁸⁾ observed intensity maxima along the v axis from their SANS results, and similar anisotropy is clear in the recent SANS data of Johnson *et al.*⁽¹³⁾

4. CONCLUSION

This paper describes a shearing cell that has been constructed for general use in a neutron facility and that has been tested at the SANS spectrometer of the National Institute of Standards and Technology. Preliminary results from a sheared colloidal suspension of 91-nm particles are presented and show very clearly the phenomenon of shear-induced melting. The sheared results differ in detail from data from light scattering⁽⁶⁾ and recent SANS experiments⁽⁷⁾ taken from polystyrene suspensions of similar particle size but different volume fractions; see, for example, Fig. 2 of ref. 7. Since the structure of the suspension, and presumably the structure changes induced by shear, are a function of volume fraction, this is not unexpected. The phenomenon of shear-induced melting needs further experimental study.

ACKNOWLEDGMENTS

Part of this work was funded by the Department of Energy, Office of Basic Energy Sciences. We are grateful to J. Gotaas of the NIST Reactor facility for his help and interest in the project. We are grateful to J. Pieper, who prepared the samples, and to B. J. Ackerson and N. A. Clark for their advice and support.

REFERENCES

1. G. C. Straty, *NIST J. Res.* **94**:259 (1989).
2. P. Lindner and R. C. Oberthur, *Rev. Phys. Appl.* **19**:759 (1984).
3. S.-H. Chen and T.-S. Lin, in *Methods in Experimental Physics*, Vol. 23, Part B, *Neutron Scattering* (Academic Press, London, 1987); R. H. Ottewill, in *Colloidal Dispersions* (Royal Society Chem. Special Publication, No. 43, 1982).
4. C. J. Glinka, D. A. Austuen, H. J. M. Hanley, and G. C. Straty, unpublished data (1989) [available from the Thermophysics Division, NIST, Boulder, 80303].
5. E. B. Sirota, H. D. Ou-Yang, S. K. Sinha, P. M. Chaikin, J. D. Axe, and Y. Fujii, *Phys. Rev. Lett.* **62**:1524 (1989).
6. R. L. Hoffman, *Trans. Soc. Rheol.* **16**:155 (1972).
7. B. J. Ackerson and N. A. Clark, *Physica* **118a**:221 (1983).
8. B. J. Ackerson, J. B. Hayter, N. A. Clark, and L. Cotter, *J. Chem. Phys.* **84**:2344 (1986).
9. H. J. M. Hanley, in *Lectures on Thermodynamics and Statistical Mechanics*, A. E. Gonzales and C. Varea, eds. (World Scientific, Singapore, 1988).
10. H. J. M. Hanley, J. C. Rainwater, N. A. Clark, and B. J. Ackerson, *J. Chem. Phys.* **79**:4448 (1983).
11. B. J. Ackerson and P. N. Pusey, *Phys. Rev. Lett.* **61**:1033 (1989); B. J. Ackerson, C. G. de Kruif, N. J. Wagner, and W. B. Russel, *J. Chem. Phys.* **90**:3250 (1989).
12. N. J. Wagner and W. B. Russel, Unpublished data (1989).
13. S. J. Johnson, C. G. De Kruif, and R. P. May, *J. Chem. Phys.* **89**:5909 (1988).
14. C. J. Glinka, J. M. Rowe, and J. G. LaRock, *J. Appl. Cryst.* **19**:427 (1986).